08

Study of capacitive and inductive elements using high-quality superconducting resonators

© *R.A. Yusupov, L.V. Filippenko, M.Yu. Fominskiy, V.P. Koshelets*

Kotelnikov Institute of Radio Engineering and Electronics, Russian Academy of Sciences,
125009 Moscow, Russia
e-mail: yusupovrenat@hitech.cplire.ru

Received May 16, 2024
Revised May 16, 2024
Accepted May 16, 2024

A method for measuring the electrical parameters of integrated circuit elements using high-quality superconducting resonators has been proposed and implemented. Structures were manufactured consisting of a coplanar waveguide line with resonators connected to it in a capacitive manner. The transmission spectra of a microwave signal along such a line were measured. A comparison is made of the numerical calculation of test structures with the transmission spectra measured in the experiment. The values of the coupling capacitances of the transmission line with the resonators are determined. The parameters of the resonator loads, which are capacitive and inductive elements, have been determined. The obtained values were analyzed and the reliability of the methodology used was assessed.

Keywords: superconducting integrated circuits, coplanar waveguide line, superconducting coplanar resonator, SQUID, SIS junction, microwave measurements, signal transmission spectrum, vector network analyzer, cryogenic measurements.

DOI: 10.61011/TP.2024.07.58806.175-24

Introduction

Creation of quantum superconducting devices is currently an important field of research [1]. Integrated circuits based on the Josephson tunnel junctions are one of the main versions of such devices [2]. Besides the Josephson junctions (JJ), such circuits often use resistive shunt, capacitive and inductive elements. Fabrication of such elements with design electric parameters is a quite difficult problem. Though the electrodynamics of such elements can be properly calculated analytically, real parameters of the fabricated elements may differ significantly from the design parameters and, therefore, need to be clarified experimentally. For example, for the circuit of Josephson traveling-wave parametric amplifier (JTWPA) based on the chain of single-contact (RF) superconducting quantum interference devices (SQUIDs) [3–7], real inductance and capacity in each cell are important to define essential parameters such as line impedance. The RF SQUID inductance includes both geometrical inductance of the SQUID loop and Josephson inductance that depends on the critical current of the tunnel junction composing the SQUID. Direct measurements of the critical current in such structures are impossible and are generally conducted in separate test structures with junctions identical to SQUID junctions. But the measurements of low critical currents equal to several μA are strongly affected by external magnetic fields and induced electrical interference, so the measured values strongly depend on the measurement system parameters.

Inductive parameters of a direct current (DC) SQUID with identical dimensions were measured before in [8]. Dependence of the critical current of such structure on the externally applied magnetic field were studied. β_L that depends on the ratio of geometrical and Josephson parts of SQUID inductance was defined from the maximum and minimum currents on the current flux curve Geometrical inductance calculated in such way depends strongly on the measurement accuracy of critical currents that are relatively low in the working structures. Thus, the DC measurements do not provide a reliable and accurate method for structures with critical currents equal to several mA. A procedure for measuring the parameters of superconducting elements within the GHz range corresponding to the operating frequency of the developed devices has been tested herein.

For RF measurement of inductive and capacitive elements they are traditionally included in an oscillating circuit with known circuit parameters. The paper discusses and uses a microwave (MW) measurement circuit using high-Q superconducting resonators loaded with the elements of interest. This method is used, first, to define the parameters of elements for which direct DC measurements are impossible, and, second, to define the necessary electric parameters on operating frequencies of the designed circuit when choosing the resonators with the required resonant frequency.

1. Measurement method using superconducting resonators

To measure the parameters of the elements of interest it is proposed to use coplanar waveguide MW resonators

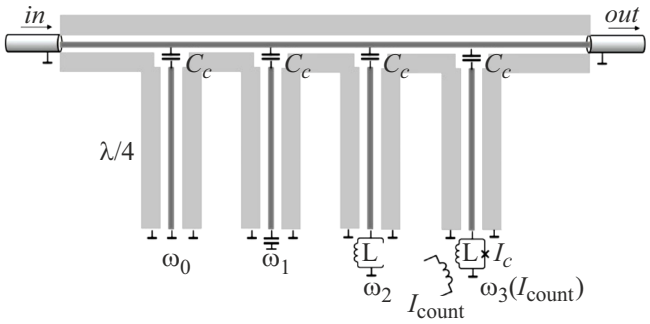

Figure 1. Connection diagram of quarter-wave coplanar resonators with different load to the coplanar line.

connected to the coplanar waveguide line via which the signal is read. Thin-film superconducting coplanar resonators are widely used in superconducting qubit circuits [9], bolometric detector matrices [10] and material analysis systems [11,12]. There are two main coupling methods for a coplanar resonator and a coplanar line: capacitive [13] and inductive [14]. The capacitive coupling option is more compact in terms of circuit design, which is very important for coupling more than one resonator with a single line. For capacitive coupling, the use of slot and interdigital capacitors is traditionally implied. In circuits with two and more metallic layers, plane-parallel capacitors may be also used to ensure much higher capacities and, therefore, the best line coupling.

The inductive and capacitive element measurement circuit is shown in Figure 1. Frequency ω_0 of a nonloaded short-circuited resonator is calculated with high accuracy analytically or by means of numerical simulation of MW devices, for example, using AWR Microwave Office. Connection of a load in form of capacity or inductance to the resonator end results in the resonator frequency shift upwards ($\omega_1 > \omega_0$) or downwards ($\omega_2 < \omega_0$), respectively. This frequency shift is also calculated analytically to determine the resonator load impedance.

A coplanar waveguide line with bonding contacts was placed on a 3×4.2 mm chip. Four coplanar resonators were capacitively coupled with this line. The central coplanar line has a length of 2500 μm, width of 20 μm and gap of 10 μm. The design transmission line impedance is equal to 48 Ω. Several types of chip designs with resonators with the same length as well as with resonators with different length pre-set to different frequencies were developed during this study. There is a problem concerning the interaction of resonators designed for closely spaced frequencies when they are connected to the same line. Therefore, one the designs initially implied that 4 resonators with different length designed for different frequencies with a step of about 500 MHz will be connected to the line. A design with the same short-circuited resonators, but with different coupling capacities was provided to determine the best coupling capacity. The main design was made in the form of a coplanar waveguide line to which four resonators with the same length (4500 μm) are connected at regular intervals through the same capacities. The end of one of the resonators is short-circuited to ground, whereas the ends of other resonators are connected to ground through the elements of interest. The circuit parameters were chosen such that to obtain a spectrum with high-Q resonances within a frequency band from 4 to 8 GHz. The circuit with elements placed on a 500 μm Si substrate ($\varepsilon = 11.9$) with a metallic layer on the back side was preliminary calculated in AWR Microwave Office.

2. Experimental sample fabrication technique

A technological facility for fabrication of micron and submicron superconducting structures based on high-quality Nb-AlO_x-Nb tunnel junctions (with a tunneling current density of $0.1-10$ kA/cm^2) is successfully used at Kotelnikov Institute of Radio Engineering and Electronics. A key feature of this technology is fabrication of complex multilayer superconducting structures with pre-defined parameters, high repeatability and multiple elements (more than 100). This technology has been adapted to fabricate samples with two superconducting layers, anodization and insulation layer to reliably prevent short circuits.

The developed design was used to fabricate the test circuits with Nb-AlO_x-Nb tunnel junctions (Figure 2). All films were deposited by magnetron sputtering, the layer structure was formed using the „lift-off“ lithography. First,

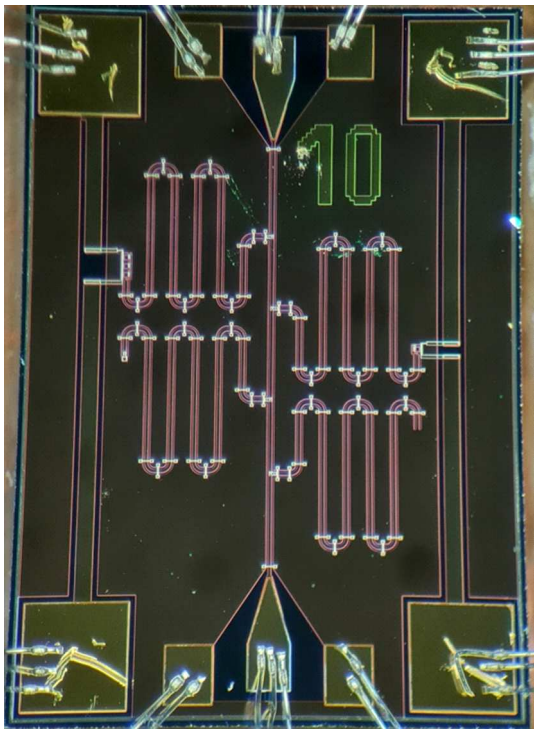

Figure 2. Photograph of the fabricated chip with 4 quarter-wave resonators capacitively coupled to the coplanar line.

a thin (100 nm) Al_2O_3 buffer layer is deposited, this sublayer is a stop layer for sandwich structure etching. The bottom metal layer where coplanar lines are made is a Nb/Al-AlO_x/Nb sandwich structure with thicknesses of 200/8/80 nm. Superconductor-insulator-superconductor (SIS) tunnel junctions in SQUIDs were formed in this layer. The junctions are formed using the SNEAP (Selective Niobium Etching and Anodization Process) technique [15]. First, a tunnel junction area is formed by etching the sandwich structure using a masking photoresist. The same resist mask is used for anodization primarily of the junction walls. Then an 250 nm SiO_2 insulator is sputtered into the areas not covered by the photoresist to ensure insulation of the bottom electrode to prevent electric contact of two superconducting layers. The 350 nm top Nb layer was used as a contactor in SQUIDs and to connect resonators to the line and create „air“ bridges. These bridges connect two ground electrodes of the coplanar line and serve for equipotential bonding of the ground busbar in bend and break points (Figure 3).

The sandwich structure formation parameters were chosen such that to achieve normal resistance $(\mathrm{RnS}) \approx 2000\,\Omega \cdot \mu\mathrm{m}^2$. The given SQUID structures use the same round Josephson junctions with diameter $d_j = 3\,\mu\mathrm{m}$ (area $S_j = 7.06\,\mu\mathrm{m}^2$). The design tunneling current step I_g on the gap voltage of the junction with a diameter of $3\,\mu\mathrm{m}$ is $7.7\,\mu\mathrm{A}$; this corresponds to the tunneling current density of $1.25\,\mu\mathrm{A}/\mu\mathrm{m}^2$ ($125\,\mathrm{A/cm}^2$). For the Nb/Al-AlO_x/Nb Josephson junctions, critical current I_c is calculated using the Ambegaokar- Baratoff equation [16] with coefficient 0.55 (to consider the strong coupling effect in Nb electrodes) and is equal to $4.2\,\mu\mathrm{A}$.

The study uses an original technique for fabrication of capacities used to couple resonators with the line. Plane-parallel capacitors with a SiO_2 insulator layer [17] separating

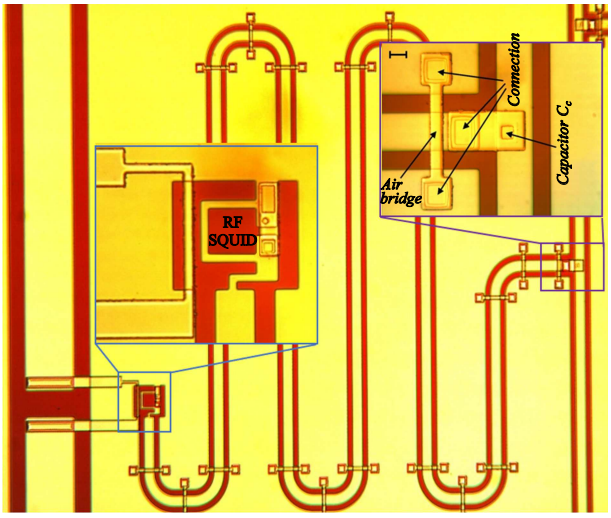

Figure 3. View of one of four quarter-wave resonators coupled capacitively with the coplanar line. This resonator is loaded with a single RF SQUID (right resonator end). The control line that sets magnetic flux in the SQUID loop through the flowing direct current is placed to the left of the loop.

the top and bottom metal layers were used before. The specific capacity of such capacitor with a 250 nm SiO_2 insulator layer was $0.17\,\mathrm{fF}/\mu\mathrm{m}^2$. For such samples, dielectric interlayer was produced by anodization of Al and Nb layers [18]. Anodization up to 17 V gives Al_2O_3 layers of about 12 nm in thickness and Nb_2O_5 layers of 18 nm in thickness. The estimated specific capacity of a capacitor with such dielectric interlayer is almost 30 times as high as that of a „standard“ capacitor with SiO_2 insulator and is equal to $5.6\,\mathrm{fF}/\mu\mathrm{m}^2$. This value may be increased by decreasing the anodization voltage or by anodization of structures with a thinner Al layer. Such method was previously proposed for capacitive shunting of the Josephson junctions [19]. The proposed technique may be used to created capacitors with high specific capacity, which is important for increasing the density of elements in superconducting circuits and creating compact multielement circuits [20]. By decreasing capacitor sizes in such circuits, spurious dimensional effects may be reduced additionally, which is necessary to ensure the MW operation of such circuits.

3. Measurement setup

The fabricated structures were measured at a cryogenic temperature of 4.2 K in a special probe insert placed into a 40l transport helium Dewar vessel. For prompt MW testing of samples, a MW sample holder, compatible with existing probe inserts and magnetic shields, was developed and made. In this MW holder, a sample is bonded to the copper base, and the electric contact is provided using ultrasonic bonding. The design has two MW lines connected via SMP connectors and 12 contacts for DC connections. The MW lines are microstrip line segments shielded on the back side, with calculated wave impedance $\approx 50\,\Omega$. A „bias-tee“ circuit option was implemented additionally to set also direct current in the MW line. For this, capacities in the form of SMD elements are built in the MW line gap and direct current is set through inductance. The MW capacity shall ensure normal transmission of high-frequency signal, but shall not have natural resonant frequencies, including during cooling to cryogenic temperature. For this, before mounting the capacities directly on the MW holder board, SMD capacities were investigated additionally in a special holder using a vector network analyzer at frequencies up to 15 GHz. It is shown that a capacity of about 100 pF is adequate for operation at frequencies from 1 GHz. Additional filters and attenuators were not used in the MW path. Signal transmission through the circuit was measured using the Rohde&Schwarz ZNB20 vector network analyzer at frequencies up to 20 GHz.

Before proceeding to resonator measurements, we performed a series of test MW measurements at frequencies up to 20 GHz. The objective of these measurements was to determine the effect of the MW feed cables, MW cryogenic insert and MW head itself on signal transmission. For correct parameter measurements, uniform signal

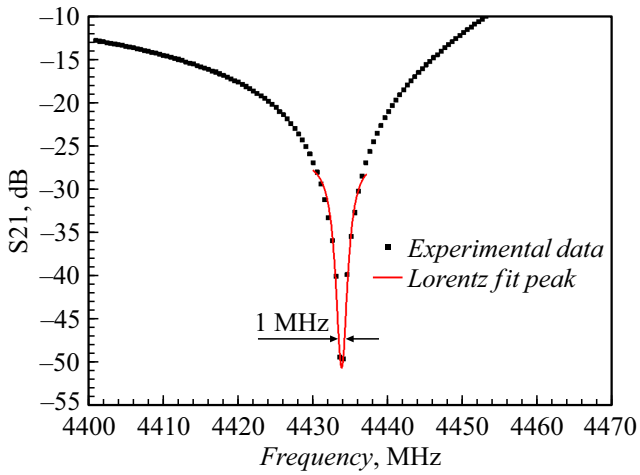

Figure 4. Experimentally measured line of one of the resonators at 4434 MHz. The width at 3 dB was 1 MHz.

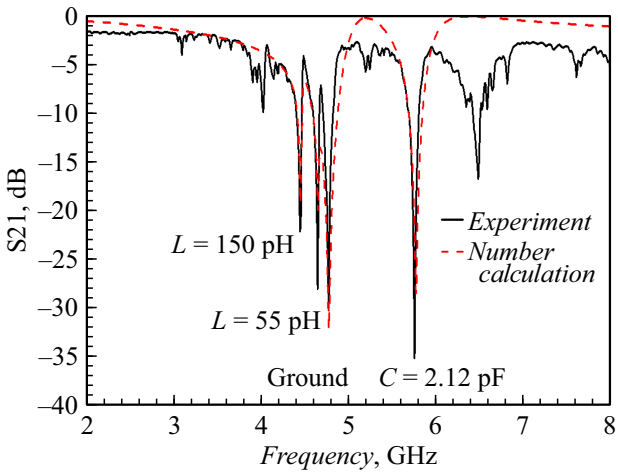

Figure 5. Experimentally measured signal transmission ratio S21 on the coplanar waveguide line of one of the samples and numerical calculation considering the bridge capacity and fitted value $C_c = 287$ fF

transmission within the given range of 4–8 GHz (without natural resonances) is required. Note that the measured signal transmission spectra at room temperatures and during cooling to the operating temperatures of 4.2 K may vary significantly; additional singularities may occur on them.

4. MW measurement data

Signal transmission ratio (S21) was measured preliminary through the identical coplanar line segment without couple resonators and no significant attenuations and reflections were found in this path. Spectra of signal transmission (S21) through the developed circuit were measured at 4.2 K. Signal power was set to the minimum value for the used vector analyzer and was equal to −30 dBm in all measurements, additional attenuators were not used. Spectra with four well-defined resonances corresponding to individual resonators were obtained. Q factor of individual resonances was more than 1000, with measurement in the frequency band 4–6 GHz of interest with resonance level up to −50 dB. Figure 4 shows one of the measured resonances and approximation of its peak by the Lorentz function. In this case, the shape of whole resonance curve differs considerable from the Lorentz curve. For scanning within the whole available range of the vector network analyzer in a wide frequency band of 100 kHz –20 GHz, the measured Q factor was more than 100 with the resonance level up to −30 dB. Q factor in such measurements depends on the resolution bandwidth defined by the resolution filter bandwidth of the analyzer that is equal by default to 10 kHz. The obtained values match with the preliminary estimates and are sufficient determine the resonance positions accurately, and ensure reliable distinguishability of resonances at closely spaced frequencies.

For comparison, a spectrum obtained by numerical calculation of the measured structure using AWR Microwave Office was overlaid on the experimentally measured spectrum (Figure 5). The calculation included all designed parameters of lines, resonators and substrate. To consider superconductivity and dielectric and radiation loss, metal resistivity normalized with respect to Au was set to 0.00001 and dielectric loss angle tangent was set to 0.001. Departure of line and resonator dimensions from the design dimensions during fabrication was negligible. First, the capacity through which the resonator and transmission line were coupled was determined using the resonance position of the short-circuited resonator. The value of this capacity consists of two components: capacity of the plane-parallel capacitor with insulator made by anodization and additional parallel capacity formed by overlapping the top and bottom metallization layers separated by the insulator layer. For sample series #32, this value was equal to 325 fF and for series #43–287 fF. These difference may be explained by different anodization conditions, which has a considerable effect on the dielectric interlayer thickness in capacitors through which the resonators are coupled. The calculation also included spurious capacity of air bridges with each of them having an estimated capacity of 20 fF.

Then, in the assumption that the coupling capacities for all resonators on one chip are identical, load impedances were selected for the calculation to ensure coincidence of the experimental and design frequency peaks. Thus, parameters of real structures in the experiment may be defined with adequate accuracy. Load capacity is a $19 \times 19\,\mu m^2$ plane-parallel capacitor made using the same technique as the coupling capacity. For series #32, specific capacity was 8 ± 0.3 fF/μm^2, for series #43–6.1 ± 0.3 fF/μm^2. Calculation and measurement using this technique are described in detail in [13].

Inductive elements represented a single RF SQUID and a circuit with three RF SQUIDs connected in series. In the absence of a magnetic field, the effective inductance of each RF SQUID is defined by series connection of the SQUID loop inductance and Josephson inductance of the junction.

Geometrical inductance values

Structure	RF SQUID 24 μm
Geometrical inductance calculated using equation1.25 $\cdot$ μ_0·d	34.4 pH
Geometrical inductanceInductEx	64 pH
DC SQUID with identical size	7 − 17 pH
RF measurements single element	65 pH−series #32 55 pH−series #43
RF measurement three elements	160 pH−series #32 150 pH−series #43

We suppose that critical current in our measurements were suppressed and inductance of such element was defined only by geometrical inductance. The table shows the calculation and measurement data for the samples from different series (substrates). For nominally identical SQUIDs in different series, their inductances shall be the same. The obtained inductances for three inductive elements are not exactly 3 times higher than for a single element, which may be explained by the contribution to inductance made by the connections and wiring. This contribution in equivalent to one element for a group of four elements is lower than for a single element. Comparison was primarily performed with the preliminary numerical calculation data of a single SQUID in InductEx. As mentioned above, the measurements of DC SQUIDs with the same sizes are not valid because there are difficulties with accurate measurement of low critical currents (I_c) and uncertainty of the modulation depth recalculation into the geometrical inductance (L_g) [3].

The effective total inductance of RF SQUID may be varied by setting various magnetic fluxes through the RF SQUID loop, thus, changing the Josephson component of inductance. For this, the design included a control line in which DC can be set (Figure 3). Magnetic field also can be set by an external coil. Such measurements require a more complex measurement setup with cold attenuators and amplifiers for circuit protection against electric noise in the MW lines that can suppress critical current in RF SQUIDs.

Conclusion

The performed measurements have shown that the developed and fabricated circuits with resonators loaded on inductive and capacitive elements are suitable quite simple experimental determination of their electric parameters. It is shown that the capacities through which resonators are coupled provide good coupling between the resonators and coplanar line in our experiment retaining quite low line width (high Q factor) of such resonances. Due to this, resonances on relatively closely spaced frequencies can be distinguished.

Values of the inductive and capacitive elements were found through the performed MW measurements. The obtained quite high specific capacity (up to 8 fF/μm^2) of the capacitor with dielectric interlayer made by anodization, makes it possible to create compact capacitors in superconducting integrated circuits, which is useful for operation of RF devices. The measured values of inductive elements were close to the numerical calculation data, which confirms the suitability of the method for the experimental determination of the parameters of the elements of integrated superconducting circuits.

Acknowledgments

The authors are grateful to A.B. Zorin for participation in this experiment, discussion of obtained results and preparation of publications.

Funding

Development and experimental investigations of the test sample were supported by grant of RSF №23-79-10262 (https://rscf.ru/en/project/23-79-10262/). Numerical calculations were supported by the Russian Ministry of Science and Higher Education of the Russian Federation (agreement № 075-15-2024-538). The samples were made using Unique Research Facility „Kriointegral“ supported within the state assignment of Kotelnikov Institute of Radio Engineering and Electronics RAS.

Conflict of interest

The authors declare that they have no conflict of interest.

References

[1] G. Wendin, Rep. Progr. Phys., **80** (10), 106001 (2017). DOI: 10.1088/1361-6633/aa7e1a
[2] R. Kleiner, D. Koelle, F. Ludwig, J. Clarke. Proceed. IEEE, **92** (10), 1534 (2004). DOI: 10.1109/JPROC.2004.833655
[3] M.T. Bell., A. Samolov. Phys. Rev. Appl., **4** (2), 024014 (2015). DOI: 10.1103/PhysRevApplied.4.024014
[4] C. Macklin, K. O'brien, D. Hover, M.E. Schwartz, V. Bolkhovsky, X. Zhang, W.D. Oliver, I. Siddiqi. Science, **350** (6258), 307 (2015). DOI: 10.1126/science.aaa8525
[5] A.B. Zorin. Phys. Rev. Appl., **6** (3), 034006 (2016). DOI: 10.1103/PhysRevApplied.6.034006
[6] A.B. Zorin. Phys. Rev. Appl., **12** (4), 044051 (2019). DOI: 10.1103/PhysRevApplied.12.044051
[7] C. Bartram, T. Braine, R. Cervantes, N. Crisosto, N. Du, G. Leum, P. Mohapatra, T. Nitta, L.J. Rosenberg, G. Rybka, J. Yang, J. Clarke, I. Siddiqi, A. Agrawal, A.V. Dixit, M.H. Awida, A.S. Chou, M. Hollister, S. Knirck, A. Sonnenschein, W. Wester, J.R. Gleason, A.T. Hipp, S. Jois, P. Sikivie, N.S. Sullivan, D.B. Tanner, E. Lentz, R. Khatiwada, G. Carosi, C. Cisneros, N. Robertson, N. Woollett, D. Duffy, C. Boutan, M. Jones, B.H. LaRoque, N.S. Oblath, M.S. Taubman, E.J. Daw, M.G. Perry, J.H. Buckley, C. Gaikwad, J. Hoffman, K. Murch, M. Goryachev, B.T. McAllister, A. Quiskamp,

C. Thomson, M.E. Tobar, V. Bolkhovsky, G. Calusine, W. Oliver, K. Serniak. Rev. Sci. Instrum., **94** (4), 044703 (2023) DOI: 10.1063/5.0122907
[8] R.A. Yusupov, L.V. Filippenko, M.Y. Fominskiy, V.P. Koshelets. Phys. Solid State, **64** (8), 467 (2022). DOI: 10.1134/S1063783422090086
[9] A. Blais, R.S. Huang, A. Wallraff, S.M. Girvin, R.J. Schoelkopf. Phys. Rev. A, **69** (6), 062320 (2004). DOI: 10.1103/PhysRevA.69.062320
[10] P.K. Day, H.G. LeDuc, B.A. Mazin, A. Vayonakis, J. Zmuidzinas. Nature, **425**, 817 (2003). DOI: 10.1038/nature02037
[11] R. Barends, H.L. Hortensius, T. Zijlstra, J.J.A. Baselmans, S.J.C. Yates, J.R. Gao, T.M. Klapwijk. Appl. Phys. Lett., **92**, 223502 (2008). DOI: 10.1063/1.2937837
[12] W. Rauch, E. Gornik, G. Sölkner, A.A. Valenzuela, F. Fox, H. Behner. J. Appl. Phys., **73**, 1866 (1993). DOI: 10.1063/1.353173
[13] M. Göppl, A. Fragner, M. Baur, R. Bianchetti, S. Filipp, J.M. Fink, P.J. Leek, G. Puebla, L. Steffen, A. Wallraff. J. Appl. Phys., **104**, 113904 (2008). DOI: 10.1063/1.3010859
[14] D. Bothner, M. Knufinke, H. Hattermann, R. Wölbing, B. Ferdinand, P. Weiss, S. Bernon, J. Fortágh, D. Koelle, R. Kleiner. New J. Phys., **15**, 093024 (2013). DOI: 10.1088/1367-2630/15/9/093024
[15] H. Kroger, L.N. Smith, D.W. Jillie. Appl. Phys. Lett., **39** (3), 280 (1981). DOI: 10.1063/1.92672
[16] V. Ambegaokar, A. Baratoff. Phys. Rev. Lett., **10** (11), 486 (1963). DOI: 10.1103/PhysRevLett.10.486
[17] R.A. Yusupov, L.V. Filippenko, D.E. Bazulin, N.V. Kolotinskiy, M.A. Tarasov, E. Goldobin. IEEE Transactions Appl. Superconduct., **32** (4), 1700105 (2022). DOI: 10.1109/TASC.2021.3131134
[18] R.A. Yusupov, L.V. Filippenko, V.P. Koshelets. Conf. Proceed. 2023 Radiation and Scattering of Electromagnetic Waves (RSEMW), **124** (2023). DOI: 10.1109/RSEMW58451.2023.10202097
[19] S. Butz, P. Jung, L.V. Filippenko, V.P. Koshelets, A.V. Ustinov, Supercond. Sci. Technol., **26**, 094003 (2013). DOI: 10.1088/0953-2048/26/9/094003
[20] J. Zotova, R. Wang, A. Semenov, Y. Zhou, I. Khrapach, A. Tomonaga, O. Astafiev, J.S. Tsai. Phys. Rev. Appl., **19** (4), 044067 (2023). DOI: 10.1103/PhysRevApplied.19.044067

Translated by E.Ilinskaya